Bull. Mater. Sci., Vol. 13, Nos 1 & 2, March 1990, pp. 113–119. © Printed in India.

Properties of gallium arsenide and indium phosphide impatts† at microwave and millimetre-wave frequencies

S K ROY and J P BANERJEE*

Centre of Advanced Study in Radiophysics and Electronics, University of Calcutta, 1, Girish Vidyaratna Lane, Calcutta 700 009, India.

*Present address: Department of Electronic Science, University of Calcutta, 92, Acharya Prafulla Chandra Road, Calcutta 700 009, India.

Abstract. The static and high frequency properties of GaAs and InP impatts have been investigated for lower microwave and higher millimetre-wave frequencies using the computer simulation programmes developed by the authors. The profiles of negative resistance and reactance in the depletion layer of SDR and DDR devices based on GaAs and InP and their admittance properties have been investigated. The results indicate that InP impatts of the SDR and DDR varieties have higher drift zone voltage, higher negative resistance and higher negative conductance as compared to their GaAs counterparts, both in the microwave frequency and in the millimetre-wave frequency ranges. It is thus observed that higher radio-frequency power can be obtained from InP devices than from GaAs devices.

Keywords. GaAs and InP impatts; microwave and millimetre-wave frequencies; Static properties; high frequency properties.

1. Introduction

During the initial phases of development of impatt devices in the late sixties and early seventies, germanium and silicon were mainly used as semiconducting materials for impatt fabrication. In view of their low power capability, Ge impatts have now become obsolete. In the seventies the rapid development of silicon technology has made possible the emergence of Si single drift and double drift impatts which can provide power at microwave and mm-wave frequency bands. GaAs also emerged as a highly suitable material for impatt action in the lower microwave frequency range (8–26 GHz). Significant improvement in the microwave performance of the GaAs impatt diode over the Si impatt diode has been achieved for frequencies ranging between C and X band up to 40 GHz. Chang *et al* (1981) reported the frequency of continuous wave (CW) oscillation of GaAs impatts at 130 GHz with a few milliwatts of power and low efficiency of d.c. to r.f. conversion. Impatt diodes have also been fabricated from another III-V material viz. InP and the first report on an SDR InP impatt performance at the *X* band became available through the work of Berenz *et al* (1978). Although the material parameters of InP are favourable for high power and high efficiency of impatts at millimetre (mm)-wave frequencies, no experimental reports are available for mm-wave InP impatts. Experimental work on GaAs impatts by Huang *et al* (1972) shows that both the power output and efficiency of GaAs impatts are quite high in the lower frequency band which fall sharply at mm-wave frequencies. These considerations have prompted the authors to investigate the d.c. and microwave properties of InP and

† Impact avalanche-and-transit time hereinafter referred to as impatts.

GaAs impatt devices for different frequencies and compare these two types of III-V materials for impatt action at lower microwave and higher mm-wave frequencies. The spatial distribution of high frequency negative resistance and reactance in the depletion layer of SDR and DDR devices and their admittance properties have been investigated. The present paper is concerned with a detailed account of these investigations.

2. Material parameters, doping profile and computational technique

The field variation of carrier ionization rates in GaAs and InP is given by

$$\alpha_{n,p} = A_{n,p} \exp\left[-B_{n,p}/E(x)\right].$$

The values of the constants $A_{n,p}$ and $B_{n,p}$ for a wide field range in GaAs for $\langle 100 \rangle$ orientation have been taken from experimental data (Ito *et al* 1978). The ionization rate constants $A_{n,p}$ and $B_{n,p}$ in $\langle 100 \rangle$ InP have been obtained from the experimental data of Kao and Crowell (1980) for the low field range ($2{\cdot}5 \times 10^7$–$5{\cdot}0 \times 10^7$ Vm^{-1}) and Umebu *et al* (1980) for the high field range ($5{\cdot}0 \times 10^7$–$8{\cdot}0 \times 10^7$ Vm^{-1}).

The negative differential mobility in the electron drift velocity versus electric field characteristics of GaAs and InP has been taken into account in the computer analysis through the expression (Kramer and Mircea 1975)

$$v_n(E) = [\mu_n E + v_{sn}(E/E_p)^4]/(1 + E/E_p)^4$$

which incorporates a peak in the drift velocity at low field (E_p) followed by a velocity saturation at high electric field.

The hole drift velocity versus field characteristics of GaAs and InP have an experimental field dependence given by

$$v_p(E) = v_{sp}[1 - \exp(-\mu_p E/v_{sp})].$$

The parameters A_n, A_p, v_{sn}, v_{sp} and E_p for two classes of III-V semiconductors viz. GaAs and InP are obtained from Bauhahn and Haddad (1977).

Realistic doping profiles for flat profile diodes have been used for the present analysis. The doping profiles at the interfaces of epitaxy and substrate are approximated by error function. The doping profile near the metallurgical junction has been made realistic by suitable experimental functions similar to those reported in Banerjee *et al* (1989).

The computation of d.c. electric field $E(x)$ and carrier current $[J_p(x) - J_n(x)]/J_0$ profiles in the depletion layer of different structures of GaAs and InP impatts has been carried out through simultaneous numerical solution of Poisson's equation and the continuity equation satisfying the appropriate boundary conditions at the edges of the depletion layer where the computation is initiated from the location of field maximum near the metallurgical junction in the depletion layer. The d.c. computer simulation method developed by the authors and reported elsewhere (Roy *et al* 1979; Datta *et al* 1982) has been used for the analytical studies of GaAs and InP impatts. The d.c. analysis takes account of mobile space charge and carrier diffusion and involves double iteration over the magnitude and location of the field maximum for proper matching of the boundary conditions for electric field and carrier current density. The d.c. profiles have been analysed to determine various

static parameters viz. avalanche zone width (x_A), breakdown voltage (V_B) of GaAs and InP impatts. A qualitative estimate of d.c. to r.f. conversion efficiency (η) of the diode has also been obtained from d.c. analysis.

A generalized computer simulation program for small signal a.c. analysis of impatts has been formulated earlier (Roy *et al* 1985) from which the profiles of negative resistance and reactance and other admittance properties viz. conductance, susceptance and quality factor can be computed. The admittance characteristics provide the overall microwave performance of the device while the negative resistance profiles provide considerable physical insight regarding the seat of microwave oscillation in the device.

3. Results and discussion

3.1 *D.C. properties of GaAs and InP impatts*

The d.c. properties of p^+nn^+ SDR and p^+pnn^+ DDR structures of both GaAs and InP impatts under identical operating conditions have been investigated for two design frequencies of 12 GHz and 65 GHz in the microwave X-band and mm-wave V-bands respectively.

Using the d.c. parameters obtained from computer analysis of the devices which have been given in table 1, a comparison of the properties of GaAs and InP impatts (both SDR and DDR) can be made for two design frequencies. The magnitudes of E_m, V_B and V_D are larger for InP impatts as compared to those for GaAs impatts for both structures under identical design frequency and operating current density. These results indicate that higher output power can be obtained from InP devices than from identical GaAs devices since InP impatts have higher breakdown voltage at a given d.c. current which leads to higher input power and coupled with higher conversion efficiency should result in higher microwave power output of InP impatts. The drift zone voltage drop (V_D) is also an indicator of higher power output since $P_{out} = P_{in} \times \eta \propto V_B \times V_D/V_B$ i.e. $P_{out} \propto V_D$ (since according to Scharfetter-Gummel semiquantitative formula $\eta = 1/\pi(V_D/V_B)$).

A comparison of the performance of SDR and DDR structures of GaAs and InP

Table 1. DC properties of SDR and DDR impatts.

Impatt based on	Structure	Design freq. (GHz)	J_0 (A/m^2)	E_m ($\times 10^7$ V/m)	X_A/W (%)	V_B (V)	V_D (V)	$\eta = (V_D/\pi V_B)$ (%)
GaAs	p^+nn^+	12	10^7	4·08	30·13	60·5	29·3	15·4
InP				5·03	30·10	76·2	39·3	16·4
GaAs	p^+nn^+	65	10^8	5·42	41·7	18·4	7·4	12·8
InP				7·21	49·3	25·8	8·8	10·8
GaAs	p^+pnn^+	12	10^7	3·66	27·3	96·6	46·7	15·5
InP				4·64	28·5	129·6	69·2	16·9
GaAs	p^+pnn^+	65	10^8	4·81	38·6	29·2	12·2	13·3
InP				5·87	34·7	35·9	17·0	15·0

$W = 3{\cdot}00\ \mu$m for SDR, $6{\cdot}00\ \mu$m for DDR at 12 GHz; $W = 0{\cdot}600\ \mu$m for SDR, $1{\cdot}20\ \mu$m for DDR at 65 GHz.

impatts designed for 12 GHz at higher level of current density can be obtained from figure 1. The current density at which the avalanche zone expands sharply is almost the same for InP and GaAs impatts. The efficiency which is proportional to V_D/V_B is found to be more sensitive to mobile space charge at higher current density for SDR InP impatts compared to that for SDR GaAs impatts (figure 1). For current density exceeding 7×10^7 Am^{-2}, the efficiency of p^+nn^+ GaAs diode exceeds that of p^+nn^+ InP-diode.

3.2 *Negative resistance profiles of SDR GaAs and InP impatts designed for the mm-wave frequency band*

The high frequency properties of GaAs impatts can be clearly understood from an analysis of the profiles of negative resistance $R(x)$ and reactance $X(x)$ in the depletion layer of the devices. These profiles are shown in figure 2 for flat profile p^+nn^+ SDR impatts based on InP and GaAs at the optimum frequencies of 60 and 70 GHz respectively for a biasing current density of 10^8 Am^{-2}. $R(x)$ profiles of the diodes exhibit one flat peak (R_{max}) in the middle of the drift layer with a negative resistance minimum (R_{min}) in the avalanche layer. The negative resistance peak for InP diode is 1·85 times higher in magnitude than that for the GaAs diode. Although microwave power is generated mainly in the drift zone, the avalanche zones of these diodes also make a significant contribution to negative resistance and microwave power. The reactance profiles exhibit capacitive maxima in the avalanche zone

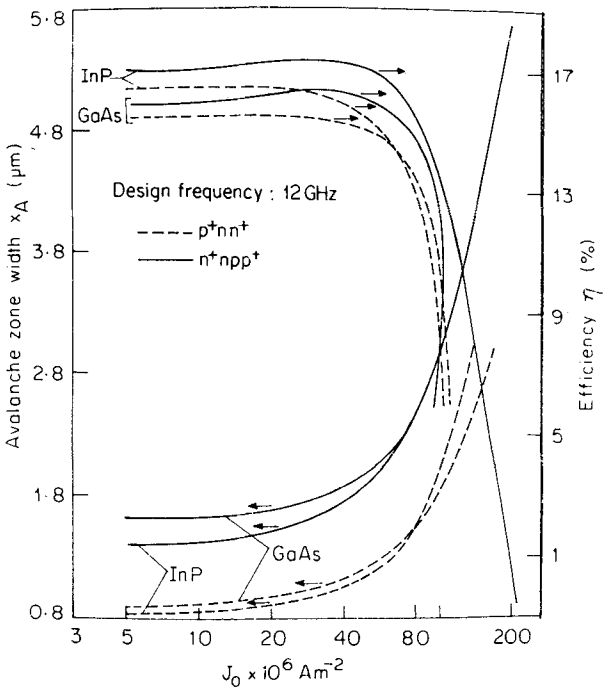

Figure 1. Avalanche zone width (x_A) and efficiency (η) vs current density (J_0) for SDR and DDR impatts based on GaAs and InP.

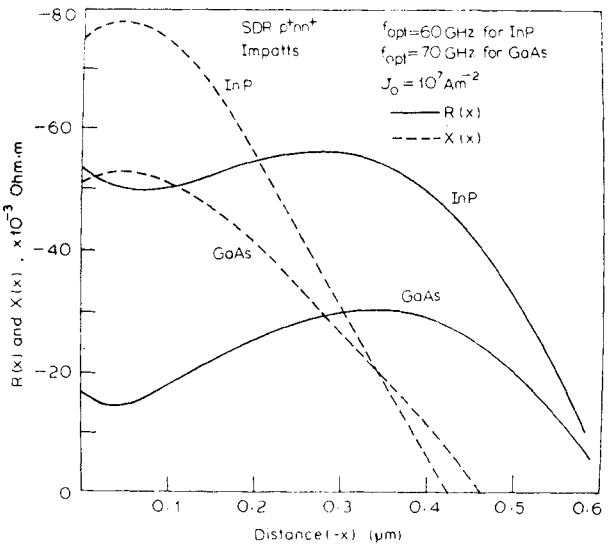

Figure 2. $R(x)$ and $X(x)$ profiles of InP and GaAs SDR impatts for mm-wave frequencies.

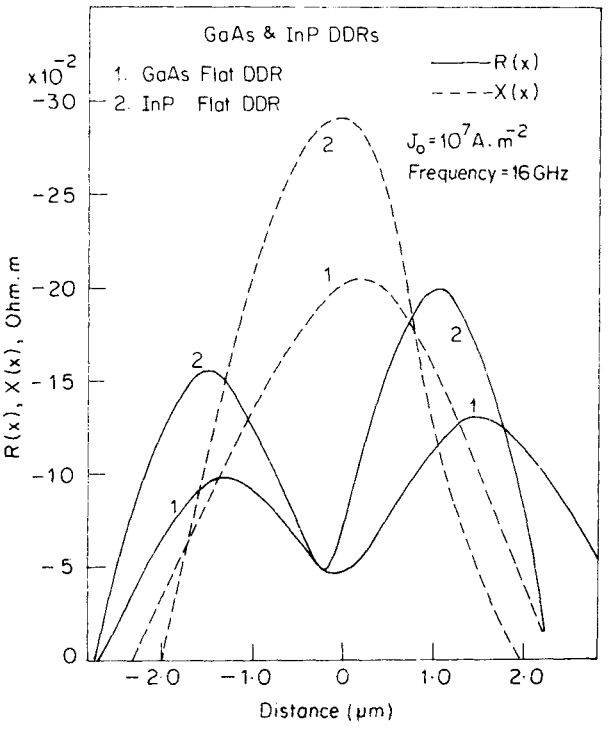

Figure 3. $R(x)$ and $X(x)$ profiles of GaAs and InP DDR impatts for Ku-band frequencies.

which falls rapidly to zero in the drift zone. The capacitive maximum is also higher in magnitude for a InP diode than for a GaAs diode.

The authors have also carried out detailed investigation on high frequency properties of DDR InP impatts for mm-wave V-band ($\sim$60 GHz) frequency for low

and high current levels from a computer simulation experiment on the profiles of negative resistance and reactance in the depletion layer which has recently been reported (Banerjee *et al* 1988). The results indicate that DDR InP devices are less sensitive to mobile space charges since there is no degradation in power output even if a high current 3×10^8 Am^{-2} is pushed through these devices. The authors have also computed the $R(x)$ and $X(x)$ profiles of DDR diodes based on GaAs and InP, both designed for 16 GHz frequency in the *Ku* band. The profiles are shown in figure 3 for an optimum current density of 10^7 Am^{-2}. The same profiles of mm-wave DDR diodes are shown in figure 4 at an optimum current density of 10^8 Am^{-2}. $R(x)$ profiles shown in figures 3 and 4 are characterised by two negative resistance peaks in the two drift layers and a central negative resistance minimum located almost at the metallurgical junction. The negative resistance peak in the hole drift layer is much larger in amplitude than the negative resistance peak in the electron drift layer for both GaAs and InP DDR diodes designed for microwave *Ku*-band and mm-wave *V*-band frequencies as shown in figures 3 and 4 respectively. For both GaAs and InP the reported experimental values of ionization rates of charge carriers indicate that holes have higher ionization rates than electrons over a wide electric field range. Thus the relative amplitudes of the negative resistance peaks in the two drift regions of DDR GaAs and InP diodes would depend on the values of ionization rates of charge carriers in the avalanche

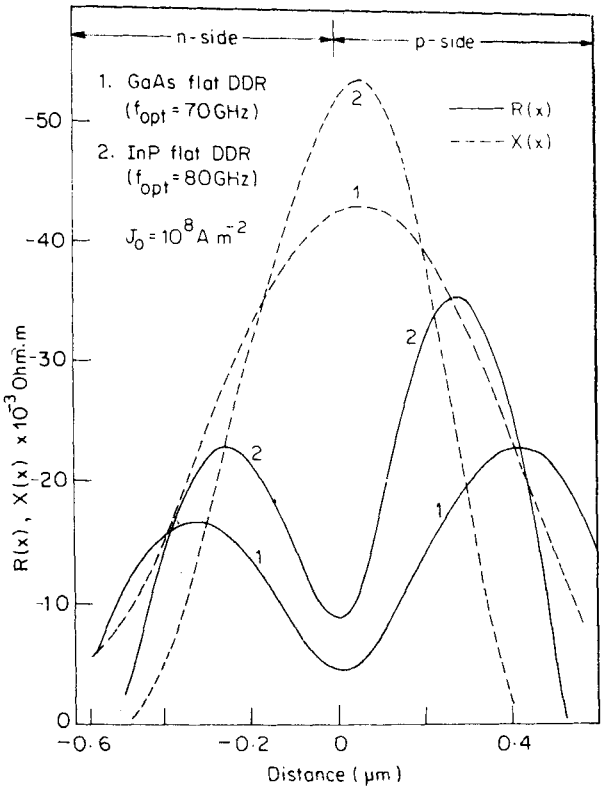

Figure 4. $R(x)$ and $X(x)$ profiles of GaAs and InP DDR impatts for mm-wave *V*-band frequencies.

zone. The correlation of the amplitudes of the negative resistance peaks with the ionization rates of respective charge carriers in the avalanche zone has been explained in a paper (Banerjee *et al* 1989) published recently. It is further observed from figures 3 and 4 that the negative resistance peaks are larger in amplitude for the DDR InP impatts as compared to those for DDR GaAs impatts designed for lower microwave and higher mm-wave frequency bands. An explanation to this phenomenon has also been given (Banerjee *et al* 1989). It has also been found that the device negative conductance and negative resistance are higher for DDR InP impatts compared to those for DDR GaAs impatts. It may therefore be seen that InP would be a highly suitable semiconductor for impatt action for both microwave and mm-wave frequency ranges in respect of power output and efficiency.

References

Banerjee J P, Pati S P and Roy S K 1989 *Appl. Phys.* **A48** 714
Banerjee J P, Pati S P and Roy S K 1988 *Phys. Status Solidi* **A109** 359
Bauhahn P and Haddad G I 1977 *IEEE Trans. Electron Devices* **ED-24** 634
Berenz J J, Fank F B and Hierl T L 1978 *Electron Lett.* **14** 683
Chang K, Kung J K, Asher P G, Hayashibara G M and Ying R S 1981 *Electron. Lett.* **17** 471
Dutta D N, Pati S P, Banerjee J P, Pal B B and Roy S K 1982 *IEEE Trans. Electron. Devices* **ED-29** 1819
Huang H C, Levine P A, Gobat A R and Klatskin J B 1972 *Proc. IEEE* **60** 464
Ito M, Kagawa S, Kaneda T and Yamoka T 1978 *J. Appl. Phys.* **49** 4609
Kao C W and Crowell C R 1980 *Solid State Electron.* **23** 881
Kramer B and Mircea A 1975 *Appl. Phys. Lett.* **26** 623
Roy S K, Sridharan M, Ghosh R and Pal B B 1979 *Proc. NASECODE-I Conf. on Numerical Analysis of Semiconductor Devices* (Dublin: Boole Press) p 266
Roy S K, Banerjee J P and Pati S P 1985 *Proc. NASECODE-IV Conf. on Numerical Analysis of Semiconductor Devices* (Dublin: Boole Press) 494
Umebu I, Choudhury A N M M and Robson P N 1980 *Appl. Phys. Lett.* **36** 302